Supplementary Information

Two-Dimensional Ferromagnetism and Driven Ferroelectricity in van der Waals $CuCrP_2S_6$

Youfang Lai[1, †], Zhigang Song[1,2, †,*], Yi Wan[1], Mingzhu Xue[1], Changsheng Wang[1], Yu Ye[1,3], Lun Dai[1,3], Zhidong Zhang[4], Wenyun Yang[1,3], Honglin Du[1], Jinbo Yang[1,3,5]

1 State Key Laboratory for Mesoscopic Physics and School of Physics, Peking University, Beijing 100871, P. R. China

2 Department of Engineering, University of Cambridge, JJ Thomson Avenue, CB3 0FA Cambridge, U.K.

3 Collaborative Innovation Center of Quantum Matter, Beijing 100871, P. R. China

4 Institute of Metal Research, Chinese Academy of Science, Shenyang 110016, P. R. China

5 Beijing Key Laboratory for Magnetoelectric Materials and Devices，Beijing 100871, P. R. China

*Correspondence: Zhigang Song (szg@pku.edu.cn)

† Those authors contribute equally to this work, and they should be viewed as first authors.

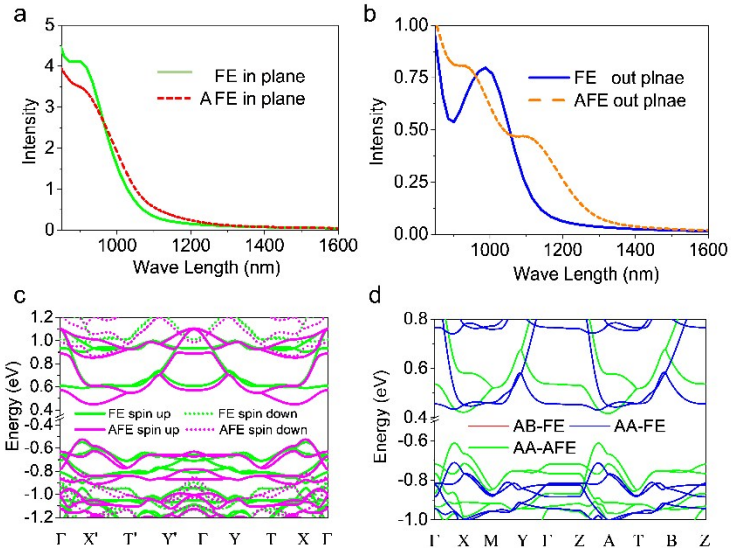

Figure.S1 (a-b) Calculated absorption spectrums of the ferroelectric (FE) and antiferroelectric (AFE) monolayers as a function of wave length of the incident light. (a) in-plane linear polarization and (b) out-of-plane polarization. (c) Spin-resolved band structures of FE and AFE monolayer $CuCrP_2S_6$. (d) Corresponding spin-polarized band structures of bulk $CuCrP_2S_6$ with interlayer antiferromagnetic ordering. Due to antiferromagnetic ordering, two spin-resolved bands are degenerate.

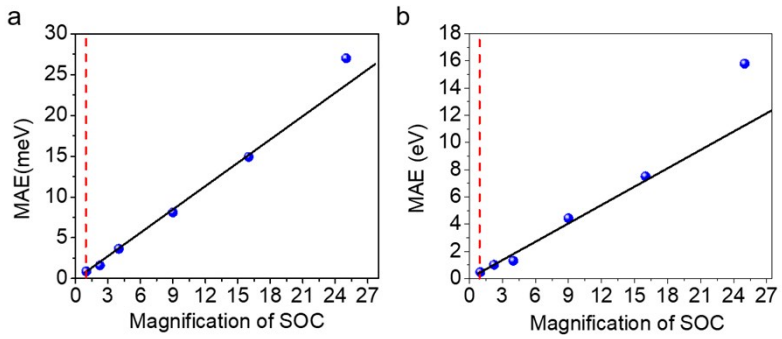

Figure S2. Magenetocrystalline anisotropy energy (MAE) as a function of spin orbital coupling. (a) Energy difference between [001] and [100]. MAE = $E_v - E_a$. (b) Energy difference between [-100] and [100], MAE = $E_{-a} - E_a$. Intercept is the real MAE, where the magnification of spin orbital coupling is 1.

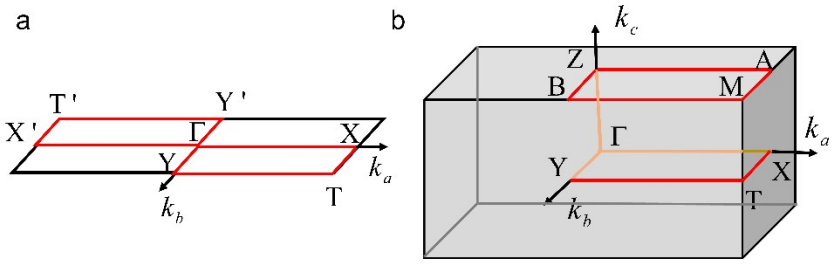

Figure. S3 High symmetric points and k-path in in the Brillouin zone of monolayer (a) and bulk (b) $CuCrP_2S_6$. Here, Γ is (0, 0, 0), X (0.5, 0, 0), Y(0, 0.5, 0), T(0.5, 0,5, 0) , X' (-0.5, 0, 0), Y'(0, -0.5, 0), T' (-0.5, -0,5, 0), Z (0, 0, 0,5), A(0,5, 0, 0,5), B(0, 0.5, 0.5), M(0,5, 0,5, 0,5).

Electric structure of $CuCrP_2S_6$ few-layers

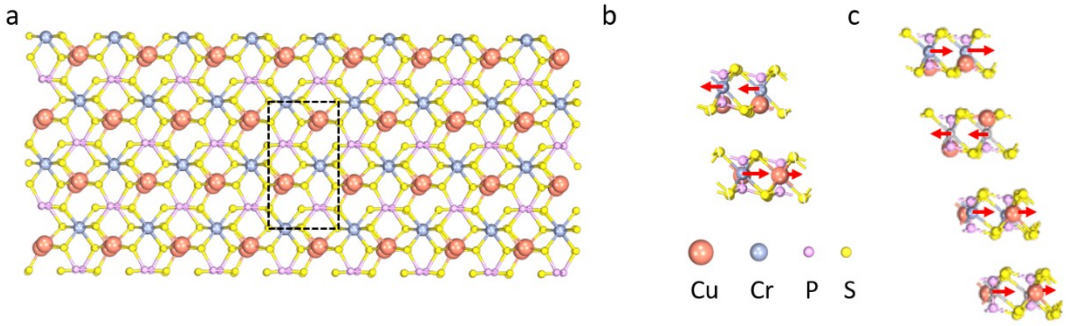

Figure.S4 Calculated $CuCrP_2S_6$ few-layers. (a) Top view of bilayer. (b) Side view of bilayer. (c) Side view of 4-layers. Red arrows represent the direction of spins. In fact, these are also sub-stable states.

Since there are ferroelectric and antiferroelectric phases in $CuCrP_2S_6$ monolayer, the possible configurations of the $CuCrP_2S_6$ few-layers are complex. Fig. S3 shows some of possible configurations, which are an optimized result in our calculations. Obtained structure of bilayer is stacked by a ferroelectric monolayer and a monolayer without electric dipole. It is antiferromagnetic and ferroelectric in total. Optimized 4-layer structure is stacked by a ferroelectric layer, an antiferroeletric layer and two layers without electric dipole. The 4-layer structure is ferrimagnetic. Thus, ferromagnetic and ferroelectric few-layers can still be observed in experiment, although the bulk is antiferromagnetic and antiferroelectric.

Preparation and characterization of bulk $CuCrP_2S_6$

The $CuCrP_2S_6$ samples are synthetized by solid state reaction of stoichiometric ratio elements, and the details are shown in the method part. The initial samples are flakes of about $0.5mm \times 0.5mm \times 1\mu m$. It can be larger if prepared by the chemical vapor transport method. Then, the structures of flakes are characterized by X-ray diffraction (XRD), as shown in Fig. S4(a). The XRD peaks are in good accordance with the previous reports,[1, 2] but our samples are strongly oriented in the (001) direction. Based on the crystal structure in previous work,[3] the lattice parameters obtained from the refinement are a=5.920(3) Å, b=10.30(1) Å, c=13.38(2) Å, β=106.7(4)°, which are close to our calculated ones. The XRD pattern shows that a small amount of phosphorus element exists in our samples, but it does not

affect the measurements of electric polarization and magnetization. Also, the electron dispersive spectrum (EDS) model of the scanning electron microscope reveals that the ratio of each elements is stoichiometric within experiment error. All the above results confirm that the sample we prepare is just what we expect. The flakes are very stable in ambient environment and room temperature and can be preserved without any protection for several months. Using an electric field of 2 kV/m, we do not observe the ferroelectricity for bulk $CuCrP_2S_6$ at room temperature by measuring the polarization of a cylinder made up by a lot of $CuCrP_2S_6$ flakes.

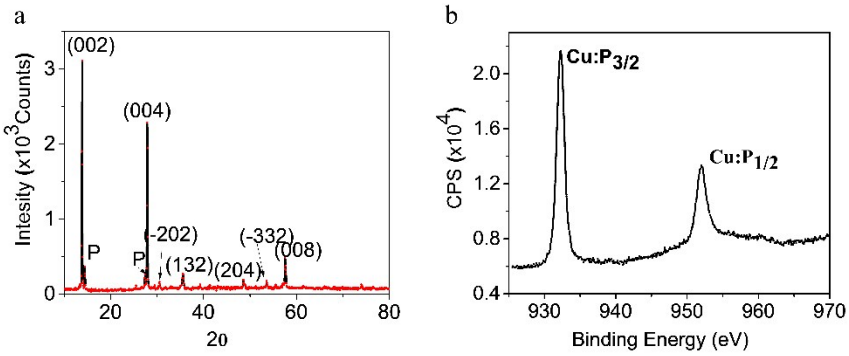

Figure S5. Structure characterization of $CuCrP_2S_6$. (a) Observed *X*-ray diffraction spectrum of the flake. (b) Cu:P peaks in X-ray photoelectron spectroscopy of the nanosheets.

Fig. S5(a) shows the thermal magnetic variation of a $CuCrP_2S_6$ flake with both parallel and vertical to the *ab* plane. Although previous work reported $CuCrP_2S_6$ bulks are antiferromagnetic below 31 K,[4] we find two differences from previous reports in our measurement. Firstly, there are cusps in the measurements both vertical and parallel to the flake. We fit the thermal magnetization curve with Curie-Weiss law $\chi=\frac{C}{T+T_\theta}$, where C is the Curie constants and T_θ is an empirical order temperature. χ and T are magnetic susceptibility and temperature, respectively. T_θ is determined to be around -25 K using data ranging from 35 K to 150 K. A negative value of T_θ and the cusp imply a stronger ferromagnetism embedded in a relative weaker antiferromagnetism. The magnetic configuration may be intralayer ferromagnetism and interlayer antiferromagnetism according to our calculation.

Secondly, the magnetic hysteresis loops vertical to the flake at 10 K exhibit typical antiferromagnetic characteristics whether the material undergoes field cooling in advance or not. When the external magnetic fields are parallel to the flake, the magnetization versus magnetic the field is non-linear in the

range of the small magnetic field. The non-linear part becomes more obvious, if the flake undergoes a field-cooling progress in advance. The nonlinear part in the magnetization curve with magnetic field is not spin flop. Firstly, spin flop is often measured in uniaxial material. Our calculation shows the material is unidirectional in the *ab* plane. Secondly, spin flop usually is independent of cooling process, if the measuring temperature of spin-flop is the same. The nonlinearity here is dependent of cooling process. Thirdly, spin flop is different when the magnetic field is rotated in the *ab* plane. However, we measure two magnetic hysterias loops using two measuring magnetic fields that have an angle of 30 degrees in the *ab* plane. They show no differences. We think the curvature could be a sign of magnetoelectric coupling rather than spin flop. Magnetoelectric coupling interaction results in a local effective field $\xi \vec{d} \times \vec{P}$, leading to a pining effect during magnetization process. During a cooling process under a magnetic field, electric dipoles are slightly oriented by magnetoelectric coupling due to the orientation of magnetic moments, and the oriented electric dipoles will be saved at low temperature. The saved configuration of electric dipoles will generate an effective magnetic field acting on spins on the magnetization process. Thus, the pining effect can be enhanced by a field-cooling progress before the measurement of the magnetization hysteresis loops. The magnetic magnetization loop after a 5 T field-cooling progress is shown in the Fig. S5(b), and the pining effect is obviously enhanced. The coupling effect only act on the in-plane spin component according to the expression of spin-orbit coupling interaction $-\xi(\vec{d} \times \vec{P}) \cdot \vec{S}$. Thus, the pining effect disappears if an external magnetic field is applied vertical to the flake to measure the out-of-plane magnetization.

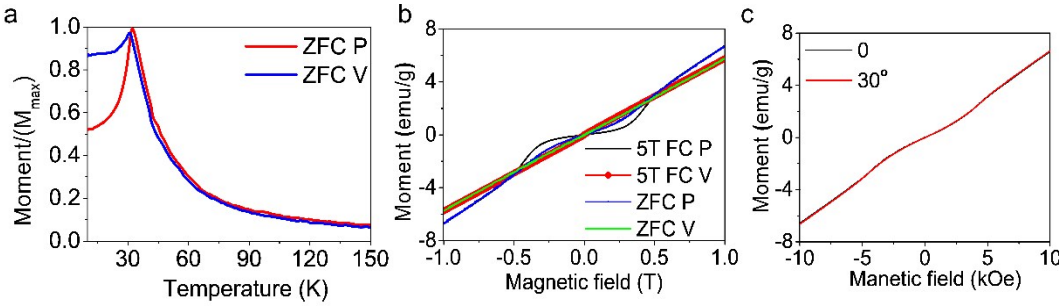

Figure S6. Characterization of magnetic properties in flakes. (a) Thermal magnetic variation of flake $CuCrP_2S_6$ with zero field cooling. M_{max} is 1.6×10^{-5} emu. (b) Magnetic hysteresis loops after the process of zero field and 5 T field cooling at 10 K. Here, P and V stands for the direction parallel and vertical to *ab* plane. ZFC and FC stands for zero field cooling and field cooling, respectively. (c) Magnetization as a function of external magnetic field applied in different angles in the *ab* plane. It is measured after ZFC process and along *ab* plane. We label the direction of first measurement magnetic field as 0 degree.

The accuracy of VSM module of PPMS is of magnitude of 10^{-7} emu. The observed values using PPMS is in the magnitude of 10^{-3} for grinded flakes and 10^{-5} emu for one flake. MOKE is characterized by the voltage on the photoelectric cell. The observed value of MOKE on exfoliated sample is 1 mV, which is beyond the limit of the MOKE. Thus, the observed hysteresis loop is sound. It is reasonable that the weak ferromagnetism is observed in very thin sample according to our first principles calculations. Similar results are also obtained in 3D $BiFeO_3$. Bulk $BiFeO_3$ is antiferromagnetic despite of intralayer ferromagnetism,[5] but a weak ferromagnetism is really observed. The reversion of spin driven by switching electric dipole is even also observed.[6]

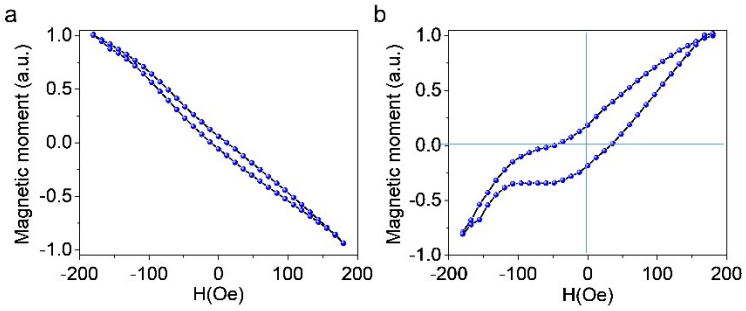

Figure S7. (a) Measured hysteresis loop of the nanosheets on a Si substrate by magneto-optic Kerr effect at 5 K. (b) Residual signal of the sample after linear subtraction of the Si substrate. In fact, the magnetic moment is measured by voltage of photoelectric cell in unit of 0.001V.

Reference

1. V. Maisonneuve, J. Reau, M. Dong, V. Cajipe, C. Payen and J. Ravez, *Ferroelectrics*, 1997, **196**, 257-260.
2. V. Maisonneuve, C. Payen and V. Cajipe, *J. Solid State Chem.*, 1995, **116**, 208-210.
3. P. Colombet, A. Leblanc, M. Danot and J. Rouxel, *J. Solid State Chem.*, 1982, **41**, 174-184.
4. W. Kleemann, V. Shvartsman, P. Borisov, J. Banys and Y. M. Vysochanskii, *Phys. Rev. B*, 2011, **84**, 094411.
5. C. Ederer and N. A. Spaldin, *Phys. Rev. B*, 2005, **71**, 060401.
6. S. Manipatruni, D. E. Nikonov, C.-C. Lin, T. A. Gosavi, H. Liu, B. Prasad, Y.-L. Huang, E. Bonturim, R. Ramesh and I. A. Young, *Nature*, 2018, 1.